Solar Energy Materials and Solar Cells 173 (2017) 50–58

Contents lists available at ScienceDirect

Solar Energy Materials and Solar Cells

journal homepage: www.elsevier.com/locate/solmat

An enhanced alneal process to produce SRV < 1 cm/s in 1 Ω cm n-type Si

Katherine A. Collett[a], Ruy S. Bonilla[a,*], Phillip Hamer[a,b], Gabrielle Bourret-Sicotte[a], Richard Lobo[a], Teng Kho[c], Peter R. Wilshaw[a]

[a] Department of Materials, University of Oxford, Parks Road, Oxford OX1 3PH, UK
[b] School of Photovoltaic and Renewable Energy Engineering, University of New South Wales, Kensington, NSW 2052, Australia
[c] Centre for Sustainable Energy Systems Engineering, The Australian National University, 32 North Road, Engineering Building, ACT 2601, Australia

ARTICLE INFO

Keywords:
Silicon photovoltaics
Surface passivation
Dielectric film
Alneal
Field effect

ABSTRACT

The *alneal* is one of the most effective methods of electrically passivating a silicon surface, and has been used by numerous research groups since the 1980s. In this work, we present an enhanced alneal process that substantially improves its effectiveness. Previously, the success afforded by the standard alneal has been attributed to the chemical passivation provided by hydrogenation of the Si-SiO_2 interface. However, the work presented here shows that it is possible to enhance the surface passivation by simultaneously introducing a component of Field Effect Passivation (FEP). Where the standard alneal is seen to provide lifetimes of ~2.1 ms, equivalent to a surface recombination velocity (SRV) of 3.3 cm/s, the enhanced alneal can provide a lifetime of 5.6 ms on 1 Ω cm, n-type Si, equivalent to a SRV 0.4 cm/s. The charge required for this enhanced passivation can be introduced in the order of minutes and has the potential to be introduced at the same time as the aluminium is deposited, thus, resulting in no extra processing time. Secondary ion mass spectroscopy showed that the nature of the charge is likely to be K and Na cations residing at the Si-SiO_2 interface. The possibility of increasing the surface passivation beyond that of the standard alneal points to the importance of both chemical and field effect components of passivation, and is therefore of significant interest to high efficiency silicon solar cell research.

1. Introduction

In the silicon solar cell industry, the efficiency of a cell is restricted by the recombination of carriers both in the bulk and at the silicon surface. To achieve high efficiency cells, this recombination must be reduced. Recombination in the bulk can be reduced using gettering techniques and/or better feedstock production [1–3], by introducing hydrogen [4,5], or by switching to n-type monocrystalline silicon [6]. However, as the bulk lifetime increases, the need to reduce surface recombination becomes more pronounced. The silicon surface is often highly recombination active due to the abundance of band-gap states that exist due to dangling bonds. The electrical effects of these defect states can be reduced by a process known as passivation. There are two passivation approaches, which are frequently used in conjunction with one another. Firstly, the number of band-gap states can be reduced by introducing a dielectric coating, which sometimes contains atomic hydrogen, and acts to saturate the dangling bonds. This is referred to as chemical passivation. Secondly, carrier access to the recombination active band-gap states situated at the silicon surface can be reduced. This is accomplished by producing an electric field that repels one type of carrier from the surface and is known as Field Effect Passivation (FEP). The *alneal*, named such by Deal [7], is one of the most effective methods of passivating the Si-SiO_2 interface [8–12]. It was characterised using photoconductance decay (PCD) effective lifetimes by Kerr and Cuevas [9], where a lifetime of 6 ms on 1.5 Ω cm n-type FZ Si was achieved. This is equivalent to a surface recombination velocity (SRV) of 1.7 cm/s, when calculated using the method reported in [13], which is briefly described in Section 2 of this paper. The *alneal* was deemed such an effective passivation technique that it was used in characterising Auger and radiative bulk recombination by Kerr and Cuevas [14]. The alneal process involves evaporating aluminium, ~ 0.1–1 μm thick, onto an oxidised silicon sample which is then annealed at 400 °C for 25–30 min [12,15], usually in forming gas (5% H_2, 95% N_2), before the aluminium is etched off in phosphoric acid at 80 °C [8,9]. It has been suggested that the passivation achieved by the alneal is due purely to chemical passivation [10,16]. The source of this chemical passivation is postulated, first by Balk [17], to be due to a reaction between the aluminium and water or hydroxyl ions present in or on the SiO_2 layer [18–22]. This reaction is reported to release atomic hydrogen that is then free to diffuse across the oxide and passivate dangling bonds at the oxide-silicon interface [10–12,16,23]. In this work, it is demonstrated that it is possible to enhance the quality of this already

* Corresponding author.
E-mail address: sebastian.bonilla@materials.ox.ac.uk (R.S. Bonilla).

http://dx.doi.org/10.1016/j.solmat.2017.06.022
Received 12 April 2017; Received in revised form 24 May 2017; Accepted 16 June 2017
Available online 03 July 2017

outstanding surface passivation by the addition of a field effect component due to the presence of Na and K ions at the Si-SiO_2 interface, where they are known to be stable [24]. Moreover, this improved passivation can be accomplished during the alneal process without the need for further processing steps.

2. Experimental methods

In this work, two sets of Float Zone (FZ), 1 Ω cm, n-type, Si wafers were used. Set A, was entirely processed at ANU. The wafers were 195 μm thick, oxidised to 140 nm at 1050 °C in dry oxygen with cooling performed in nitrogen. The other set, set B, were 200 μm thick, oxidised to 100 nm in oxygen and dichloroethylene at 1050 °C at Fraunhofer ISE. The alneals were carried out in two separate laboratories. For set A, which achieve standard alneal results, the full 4″ wafer was coated on both sides with 100 nm 99.999% purity aluminium, thermally evaporated using a tungsten boat. The alneal for these wafers was done at ANU in forming gas at 400 °C for 30 min. After oxidation, set B wafers were entirely processed using the Materials Department semiconductor cleanroom at Oxford. These wafers were cleaved into 3 × 3 cm^2 lifetime samples before ~ 100 nm of 99.999% purity aluminium was thermally evaporated onto both sides using a tungsten coil. Sample set B was alnealed in a tube furnace under an argon atmosphere at 400 °C for 30 min. The use of two different gas ambients at ANU and Oxford should have little effect on the passivation achieved as noted in Ref [20]. After the alneals, the aluminium in set A was etched off using warm (≤ 80 °C) phosphoric acid, and in set B using commercial aluminium etchant (phosphoric acid 60%, acetic acid 3.5%, nitric acid 2.5%). It will be shown that set A samples exhibited behaviour typical of other alneal results reported in the literature whilst set B samples exhibited markedly improved performance. The set A and B samples will subsequently be referred to as “standard” and “enhanced” alneal respectively. A small quantity of Cz, ~40 Ω cm, n-type silicon, oxidised to 100 nm was also used for aluminium anneals. These are not referred to as alneals because the samples were smaller than appropriate for lifetime measurements and therefore aluminium was only deposited on one oxide surface prior to the anneal, as is adequate to measure interface charge using capacitance-voltage. These samples were thermally oxidised in the semiconductor cleanroom at Oxford to 100 nm in a pure oxygen atmosphere, with a nitrogen cool.

Sinton photo-conductance decay (PCD) measurements were taken to calculate the effective lifetime of the silicon specimens. All lifetime values are quoted at an injection level of 10^{15} cm^{-3} unless indicated otherwise and taken at 25 °C. Once an effective lifetime measurement has been made it is common to convert this into a surface recombination velocity (SRV). This describes how effective a surface is as a recombination site. The lower the value, the less recombination occurs and the better the passivation. This parameter is useful when discussing surface passivation as, unlike lifetime results, it is independent of sample thickness and, under certain circumstances described by McIntosh and Black [25], independent of doping concentration. Luke and Cheng [26] showed that the SRV can be considered as a function of the sum of decaying exponential terms of effective lifetime. The dominant term is the first mode. From equation A7 in [26] or Eq. (2) in [27] SRV can be calculated as:

$$SRV = \sqrt{D\left(\frac{1}{\tau_s}\right)}\, tan\left(\frac{W}{2}\sqrt{\frac{1}{D}\left(\frac{1}{\tau_s}\right)}\right) \quad (1)$$

where W is the wafer thickness, D is the ambipolar carrier diffusion coefficient and τ_s is the surface lifetime as described by:

$$\frac{1}{\tau_{eff}} = \frac{1}{\tau_b} + \frac{1}{\tau_s} = \frac{1}{\tau_{rad}} + \frac{1}{\tau_{Aug}} + \frac{1}{\tau_{SRH}} + \frac{1}{\tau_s} \quad (2)$$

where τ_{eff} is the effective lifetime, measured by the Sinton lifetime tester, and τ_b is the bulk lifetime. The bulk lifetime comprises three lifetimes, determined by three types of recombination: radiative τ_{rad}, Auger τ_{Aug} and defect mediated, the latter is characterised by Shockey-Reed-Hall statistics τ_{SRH}. Richter's parameterisation [28] is used to calculate the Auger and radiative recombination, using coefficients for radiative recombination as defined in [29,30]. As monocrystalline n-type FZ silicon is used for all lifetime measurements in this work, the defect mediated recombination was assumed negligible for SRV calculations. In order to calculate D, Klassen's mobility model [31] was employed using the online calculator of PV Lighthouse [32].

Another metric used to characterise how good a dielectric is at passivating the silicon surface, is the emitter saturation current density (J_{0e}). J_{0e} represents the loss due to recombination in the emitter and at the surface. However, in this work surface saturation current density (J_{0s}) values are quoted, as there is no emitter present. In recent work by McIntosh and Black [25], they report that J_{0s} is independent of doping concentration for the majority of practical conditions. For this reason, it may even be considered to be a preferable metric for surface passivation than SRV. J_{0s} has been calculated based on Mäckel and Verner's work [33] and using an iterative algorithm as proposed by Kimmerle et al. [34], and also detailed in reference [13], with the effective intrinsic concentration is calculated using Pässler's model [35] implemented online by PV lighthouse [32].

As mentioned in the introduction, there are two forms of surface passivation, chemical and field effect. Chemical passivation is quantified by the density of surface states, otherwise termed interface traps (D_{it}), and the relative capture cross sections of such traps. The density of interface traps is a measure of how many trap levels exist in the forbidden band-gap. These trap levels are caused by defects, such as dangling bonds, and act as recombination centres for holes and electrons. As chemical passivation is introduced the density of interface traps decreases, or their capture cross section reduces. The density of traps D_{it} varies across the band-gap, thus is an energy-dependant quantity with units eV^{-1} cm^{-2}. It is convention to quote the density of interface states at mid-gap as this is where the most effective recombination traps lie. In this work, D_{it} is calculated using the Terman [36] high frequency CV method. However, this technique is known to be relatively inaccurate, so the D_{it} values reported may only approximate the true values [37]. For a Si-SiO_2 interface, the capture cross sections are well characterised for both as-oxidised and alnealed interfaces. The capture cross section varies with trap energy and reports of these values can be found in section 4.2 of Ref [16].

Field effect passivation is provided by charge in the dielectric. Charge residing anywhere in the dielectric produces a space charge region at the surface of the silicon, causing the bands to bend and one carrier type to be repelled from the surface. This reduces access of that carrier type to the recombination active interface traps, and thus lessens recombination at the surface. Two techniques are used to measure dielectric charge density directly. Kelvin Probe is used to infer charge near the surface of the dielectric using measurements of surface potential, and the capacitance-voltage (CV) technique enables charge at, or close to, the Si-dielectric interface to be calculated from flatband voltage shifts. These two techniques, and the way in which the measurements can be used in conjunction with one another to locate charge within the dielectric, are explained in Ref [38]. CV measurements were taken either using the mercury probe (Hg-CV) technique or an Al dot of 2 mm diameter, thermally evaporated through a mask. Both types of passivation, chemical and field effect, will cause an increase in the sample lifetime. However, it is valuable to know which type of passivation the lifetime increase is due to. Identifying this may enable appropriate, cheap, effective passivation techniques to be developed. From a lifetime measurement alone, it is not evident which type of passivation is responsible for the increase in lifetime, hence, there is the need for D_{it} and dielectric charge calculations.

Thermally Stimulated Ionic Conduction (TSIC) measurements were used to quantify the concentration of ions that migrate across the oxide at elevated temperature under an external bias. For these

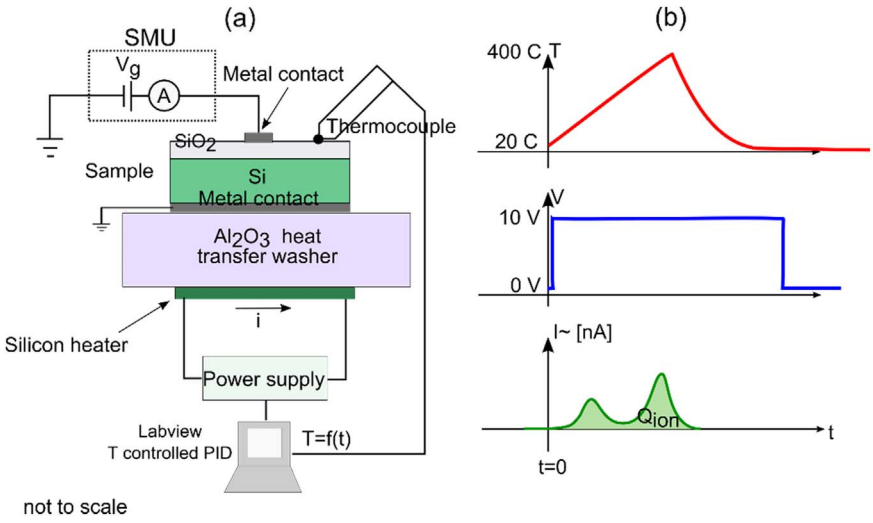

Fig. 1. Thermally Stimulated Ionic Conduction (TSIC) (a) schematic and (b) typical measured parameters during the experiment.

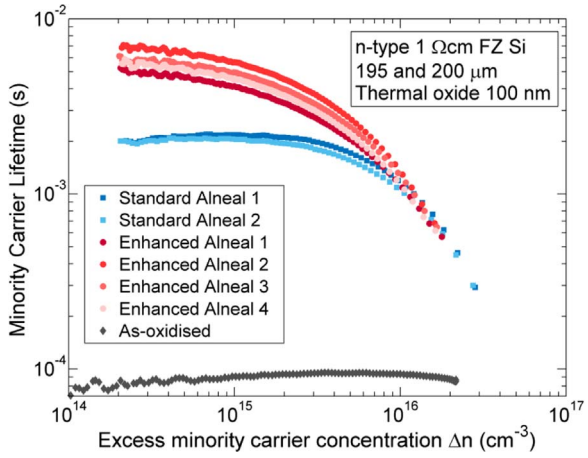

Fig. 2. Injection level dependant lifetimes of standard alneal, enhanced alneal and as-oxidised samples. The numbers associated with the standard and enhanced alneal samples are for sample identification.

measurements, a metal-oxide-silicon (MOS) structure was required. The metal front contact and silicon then act as electrodes that a voltage can be applied between. This results in a voltage drop across the MOS, which can be applied at elevated temperature in air ambient. The current between the two electrodes is monitored while the voltage is applied by use of a source measure unit (SMU). This enables the migration of ions, which produce an electrical current, across the MOS structure to be recorded. Thus, TSIC experiments allow the magnitude of this current to be characterised as a function of temperature, applied bias and time. The set-up is shown in Fig. 1. For these experiments, MOS capacitor samples were prepared by removing the back oxide using HF and evaporating aluminium onto the bare silicon to create a back contact. The front contact was created by evaporating a metal dot of 2 mm diameter through a contact mask onto the SiO_2. A voltage was applied between the silicon bulk and the top metal dot while the sample was on a hotplate and the temperature controlled. The voltage continued to be applied as the sample cooled to minimise diffusion of the ions back to their original position. The current between the contacts was recorded using LabVIEW. This current reading could then be integrated, with respect to time, and used to calculate the movement of charge between the two electrodes. At the temperatures used, and with the voltages applied, other current mechanisms were found to be one or two orders of magnitude smaller than the measured current when ions were present. Thus, in this work, the measured current is approximated to be due entirely to the migration of ionic charge through the MOS structure and the charge concentration calculated from the integral of the current is taken to be equivalent to the charge migrated to the Si-SiO_2 interface. In addition, CV measurements of the samples after TSIC processing were made as an independent measurement of the Si-SiO_2 interface charge. The hot plate was also used for anneals on some small samples. Unlike the lifetime samples, that were annealed in the tube furnace under argon ambient, the hotplate anneals were completed under an air ambient. The temperature of the hotplate was monitored and controlled via a LabVIEW software. A K-type thermocouple, placed next to the sample, measured the temperature. This was recorded by the LabVIEW software and controlled via a PID using the thermocouple as the sensing element.

3. Effective lifetimes in enhanced alneal processed material

The standard alneal process is known to provide one of the most recombination inactive Si-SiO_2 interfaces [9,13,14]. In the literature, the highest quality alneal is reported to achieve an SRV of 1.7 cm/s [9,13]. This already shows a substantial reduction in the recombination activity of the interface compared to an as grown Si-SiO_2 interface. A typical, thermally grown oxide-silicon interface would produce a SRV of 50–150 cm/s [39,40]. In this work, alneal samples with exceptionally high lifetimes are reported. As mentioned in Section 2, these are referred to as enhanced alneal samples due to the enhanced surface passivation. Fig. 2 shows the injection level dependant lifetimes for two standard alneal wafers (experimental set A) and four enhanced alneal samples (experimental set B). An as-oxidised sample from the specimens used for the enhanced alneal is shown for comparison.

The highest lifetime achieved by an enhanced alneal sample was 5.6 ms at $\Delta n = 10^{15}\,cm^{-3}$. This is equivalent to a SRV of 0.4 cm/s. Considering the size of this sample ($3 \times 3\,cm^2$), the lifetime was likely limited by edge, rather than by surface, recombination [41]; thus implying the actual SRV could be significantly less. In comparison, the standard alneal wafer achieves a lifetime of 2.2 ms, the equivalent to a SRV of 3.3 cm/s which is believed typical of standard alneal material [40,42]. The high lifetimes achieved by the enhanced alneal are unprecedented and understanding the type of surface passivation producing them is therefore of significant importance.

Previous works have concluded that the effectiveness of the alneal is entirely due to chemical passivation [10,23]. The dielectric-silicon interface chemistry has been routinely characterised by its density of states $D_{it}(E)$. However, in the well-accepted Shockley-Read-Hall (SRH) [43,44] theory of defect-mediated recombination, the effectiveness of the interface as a recombination site is in fact characterised by the energy-dependant electron capture velocity $S_n(E) = v_{th} D_{it} \sigma_n$, and hole capture velocity $S_p(E) = v_{th} D_{it} \sigma_p$, where σ represents the capture cross

section of the states, and v_{th} the thermal velocity of the carriers. Chemical passivation thus aims to reduce both the D_{it} and $\sigma_{n,p}$ for a particular dielectric-silicon interface. A theoretical evaluation using SRH theory has been performed here to estimate the effective lifetimes expected from the standard alneal as reported by Eades [45], and Kerr and Cuevas [9], considering the up-to-date parametrisation for bulk lifetime in silicon reported by Richter [28]. An excellent estimate can be achieved by assuming a uniform density of interface states for all energies, here referred to as D_{it} for simplicity. This approximation helps to compare the D_{it} parameter used in modelling, with the mid-gap D_{it} commonly measured and quoted in the literature. The effective lifetime is then calculated as [46–48]:

$$\frac{1}{\tau_{eff}} = \frac{1}{\tau_{Rad}} + \frac{1}{\tau_{Aug}} + \frac{2S_{eff}}{W} = \frac{1}{\tau_{Rad}} + \frac{1}{\tau_{Aug}} + \frac{2}{\Delta n_d W}\int_{E_V}^{E_C} \frac{(n_s p_s - n_i^2)}{[(n_s + n_i e^{E/kT})/S_{p0} + (p_s + n_i e^{-E/kT})/S_{n0}]} dE \quad (3)$$

where τ_{Rad} is the minority carrier lifetime subject to radiative recombination, τ_{Aug} is the minorty carrier lifetime subject to Auger recombination $S_{p0,n0}$ are the energy independent surface recombination parameters of holes and electrons at mid-gap, n_s is the carrier concentration at the silicon surface and Δn_d is the excess minority carrier concetration at depth d, the depth at which any surface charge has a negligible effect on band bending. An algorithm, based on work by Girisch et al. [47] and Aberle et al. [48], was used to solve Eq. (3). The algorithm incorporates the contribution from photo-generated carriers, and accounted for dielectric film charge located anywhere in the dielectric Q_f, the silicon surface space charge region $Q_{Si}(n_s, p_s)$, and charged interface states Q_{it}. Fig. 3 illustrates the solution to Eq. (3) using this algorithm for a typical alnealed Si-SiO_2 interface. Several studies have been performed on the Si-SiO_2 interface to determine the D_{it} and $\sigma_{n,p}$. Here, a range of D_{it} mid-gap values have been used to exemplify the typical and lowest reported in the work of Eades [45] and Nicollian [37], while $\sigma_{n,p}$ have been taken as typical as reported by Aberle [16].

According to the extended-SRH model, in the absence of additional FEP, with a low film charge concentration of $Q_f = 10^9$ q/cm^2, a lifetime of 5.6 ms (as the enhanced alneal) would require a D_{it} below 10^9 eV^{-1} cm^{-2}. Eades [45] and Aberle [16] report some of the lowest values of D_{it} for alnealed Si-SiO_2 interfaces in the range of 1–5 × 10^9 eV^{-1}cm^{-2}. From this, it is extremely physically unlikely that a

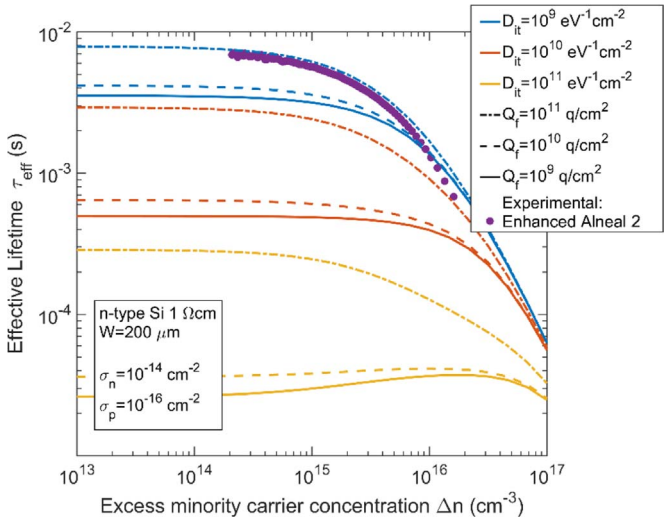

Fig. 3. Simulated injection level dependant effective lifetimes showing D_{it} mid-gap values for an alnealed interface (typical, 10^{10}–10^{11} eV^{-1} cm^{-2}, and extreme, 10^9 eV^{-1} cm^{-2}) [5,10,14,36] and dielectric film charge Q_f for an as-grown thermal silicon dioxide (typical, 10^9 to 10^{10} q/cm^2, and extreme, 10^{11} q/cm^2) [16].

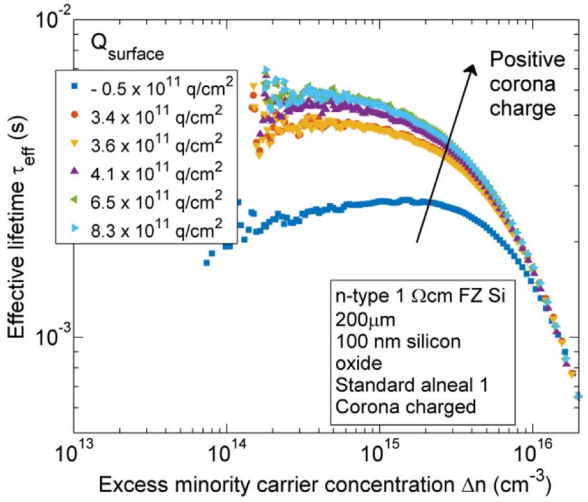

Fig. 4. Injection dependant effective lifetimes for standard alneal 1 with the addition of positive charge to the oxide surface ($Q_{surface}$) from corona.

$D_{it} < 10^9$ ev^{-1}cm^{-2} would be characteristic of the samples used for the enhanced alneal. Especially as these samples did not undergo a post oxidation high temperature anneal in argon as the samples used by Eades and Aberle. Even if the enhanced alneal samples were to have an extremely low density of interface traps (10^9 eV^{-1} cm^{-2}), the modelling in Fig. 3 shows that an aspect of FEP would be necessary to achieve the lifetimes reported. This indicates that the enhanced alneal passivation is likely to be due to the presence of dielectric charge, and that this charge is responsible for the substantial difference in lifetime of the standard and enhanced alneal.

To investigate the impact of increasing dielectric film charge concentration (Q_f) on alnealed samples, one of the standard alneal samples was cleaved into a quarter wafer and corona charge [38] was deposited onto both oxidised surfaces of the sample in incremental steps. After each deposition, both the effective lifetime of the sample was measured and a KP measurement was taken to calculate the surface charge density of the corona deposition. The effective lifetime variation with dielectric surface charge is shown in Fig. 4.

From Fig. 4 it is clear that the addition of FEP is indeed capable of improving the lifetime of a standard alneal specimen. By increasing the oxide surface charge to +8.3 × 10^{11} q/cm^2, the effective lifetime at $\Delta n = 10^{15}$ cm^{-3} improves from 2.65 ms to 5.35 ms. This increase is the equivalent to the SRV reducing from 2.4 cm/s to 0.5 cm/s. This latter SRV shows a significant improvement on any SRV reported solely due to the standard alneal process and reiterates that FEP can improve the passivation, already considered high quality, of the alneal. In fact, the lifetime achieved by the standard alneal with the addition of FEP corona charge is equal to that of the enhanced alneal, 5.35 ms and 5.64 ms respectively. This reinforces the hypothesis that there is charge present in the enhanced alneal that is facilitating such a high lifetime and low SRV.

4. Passivation mechanisms in the enhanced alneal

The enhanced alneal samples shown in Fig. 2 were characterised to establish whether there was charge present in the dielectric. Both CV and KP measurements were taken to calculate Q_f -the total concentration of dielectric charge. In all cases, the KP measurements were found to be negligible, indicating insignificant charge near the surface of the oxide. Therefore, the Q_f obtained has been referred to here as the charge at the Si-SiO_2 interface $Q_{interface}$. It was found that CV measurements of $Q_{interface}$ differed between the standard alneal and the enhanced alneal. For the standard alneal samples, the interface charge was within the typical range of an as-oxidised Si-SiO_2 interface (5 × 10^{10} to 2 × 10^{11} q/cm^2 [16]), with a charge concentration of ~6 × 10^{10} q/cm^2.

Table 1
Alneal samples τ, J_{0s}, D_{it} and $Q_{interface}$.

Batch	τ (μs)	SRV (cm/s)	J_{0s} (fA/cm^2)	D_{it} (eV^{-1} cm^{-2})	$Q_{interface}$ (q/cm^2)
As-oxidised	90	112	1.3	1×10^{11}	2×10^{11}
Standard Alneal 1	2169	3.3	1.6	1×10^{11}	5.9×10^{10}
Standard Alneal 2	2049	3.5	2.4	–	–
Enhanced Alneal 1	4094	1.1	4.6	3×10^{11}	1.4×10^{12}
Enhanced Alneal 2	5643	0.4	2.1	3×10^{11}	1.7×10^{12}
Enhanced Alneal 3	4917	0.7	3.8	1×10^{11}	1.3×10^{12}
Enhanced Alneal 4	4548	0.9	4.2	1×10^{11}	1.1×10^{12}
TSIC Enhanced Al dot	–	–	–	–	1.3×10^{13}

Whereas, for the enhanced alneal samples, the interface charge calculated from CV measurements was over an order of magnitude higher at ~10^{12} q/cm^2. It is thus concluded that the anomalously low SRV values provided by the enhanced alneal are due to the presence of increased interface charge, which is absent in standard alneal specimens. This indicates that the increased charge is able to enhance greatly the passivation provided by a standard alneal.

The characteristics of both the standard and enhanced passivation samples are presented in Table 1. The techniques used to calculate the reported values are described in Section 2. Before the enhanced alneal treatment, the samples showed an interface charge of ~ 2×10^{11} q/cm^2 and a D_{it} of ~ 10^{11} cm^{-2} eV^{-1}. It should be noted that the Terman method was used to calculate D_{it} so the values reported should be considered only to approximate the true value.

It was hypothesised that the increased interface charge was due to the presence of ionic contaminants that were present for the enhanced alneal specimens but were not present in the standard alneal specimens. As the density of silicon surface atoms is ~ 7×10^{14} cm^{-2} [16], this concentration of interface ions would represent only ~2×10^{-3} of a monolayer and appears not to compromise chemical passivation. This was tested by TSIC measurements at 300 °C with a 5 V bias performed using an aluminium front contact deposited in the same laboratory (Oxford) as the enhanced alneal specimens. The TSIC showed an ionic drift current and resulted in a further increase in interface charge, as shown in Table 1. Due to the small area of the TSIC process, these specimens could not be used for lifetime measurements. The magnitude of charge introduced also discounted the possibility of D_{it} analysis as it was beyond the equipment measurement range. It is likely that during the enhanced alneal, some of the ions, which are assumed to be responsible for the interface charge, diffuse through the oxide to the interface. However, when TSIC is performed a greater number of ions are able to reach the interface because the applied electric field provides a larger driving force for ionic migration than diffusion alone.

Once interface charge was identified from CV measurements, the cause of the charge was investigated. It was assumed to be an ionic species at the Si-SiO_2 interface and thus SIMS measurements were conducted at Aystorm Scientific Ltd. Due to limitations of equipment sensitivity, these measurements were only performed on the enhanced alneal specimens that had undergone TSIC. The SIMS results are displayed in Fig. 5 and show that both sodium and potassium are present at the Si-SiO_2 interface. Note that the broadening of the impurity peaks across the Si/SiO_2 interface can be an artefact of the technique.

The predominant impurity elements detected were sodium and potassium as shown in Fig. 5. Previous work has shown that, when intentionally contaminated via thermal evaporation of salts, it is possible to diffuse, or drift, both of these ions into a thermally grown SiO_2 film where they will reside at the Si-SiO_2 interface in a charged state [49]. However, for this sample, no intentional Na or K contamination had occurred. In addition, Fraunhofer ISE who performed the oxidation had no evidence of contamination occurring during that process. CV measurements on samples which had not undergone an anneal after aluminium deposition also showed no interface charge. Such charge

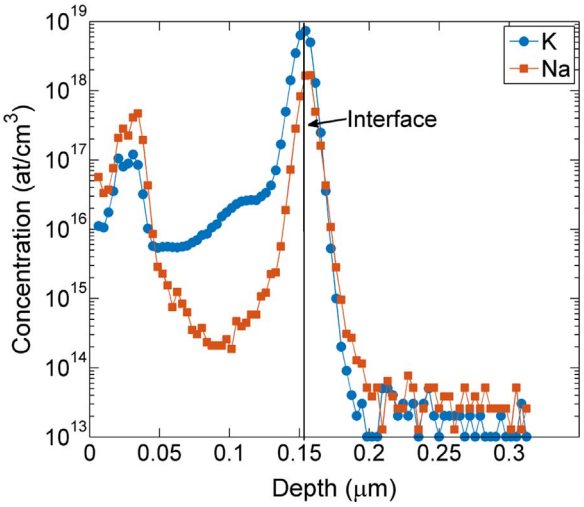

Fig. 5. SIMS results of sample, with an Al front contact deposited at Oxford, having undergone TSIC at 300 °C with a 5 V bias. SiO_2 on the left, and Si on the right, of the marked interface.

appeared only after aluminium deposition and annealing (in the Oxford cleanroom). Since other processes conducted in this cleanroom use Na and K; it is thought that these will be the source of the metal contamination which then becomes mobile during the anneal and are responsible for the interface charge detected in the enhanced alneal samples.

From the SIMS data it is possible to calculate the cumulative charge per unit area within the dielectric. This is done by integrating the concentration (at/cm^3) of K and Na detected by the SIMS data with respect to depth. The initial peak on the left-hand side of the SIMS results is disregarded in this calculation as it is an artefact of the measurement and the integration is done for the peak at the marked interface between a depth of 0.1 μm and 0.18 μm. For the sample in Fig. 5, that had not been intentionally contaminated with salts, this calculation revealed that the concentrations of Na and K near the interface were 1.9×10^{12} at/cm^2 and 9.3×10^{12} at/cm^2, respectively; which gives a cumulative concentration of 1.12×10^{13} at/cm^2. This is similar to the value of charge inferred from the CV curve, which was 1.3×10^{13} q/cm^2, which is in agreement with the migrated charge calculated from the TSIC current data, which is also 1.3×10^{13} q/cm^2. This similarity in concentration of Na and K from SIMS and charge concentration from TSIC and CV gives reason to believe that the Na and K atoms are ionic species responsible for the interface charge. The fact that Na and K are known to reside at the Si-SiO_2 interface as charged ions, and the similarity in charge and contaminant concentration corroborate the theory that the charge is due to ionic species that have now been identified. This also indicates that all Na and K ions at the interface are in a +1 charged state. Alkali ions present at the Si-SiO_2 interface have been reported to produce a charge which is effectively stable for time periods in excess of 3 years and perhaps indefinitely [24,49]. The discovery that ionic Na and K can be introduced during the alneal process, to enhance the surface passivation of the alneal via FEP, which holds promise to be stable for the lifetime of the solar panel, is of significant importance to both research and industry.

In recent years, a wide number of extremely effective passivation methods have been proposed, especially with the advances on plasma enhanced CVD and atomic layer deposition (ALD) methods. Table 2 illustrates a comparison of the surface recombination velocities for the enhanced alneal and other high quality passivation techniques, as well as the best recorded standard alneal. From these calculated SRVs, it is clear that the effectiveness of the enhanced alneal is among the highest achieved for a ~1 Ω cm n-Si surface. It is to note that the enhanced alneal is capable of producing surface passivation superior to the best silicon nitride capping layer. However, it is not as effective as the ALD

Table 2
Summary of best passivation achieved by several high quality passivation dielectrics.

Dielectric	Passivation	Type	Resistivity (Ω)	SRV (cm/s)
SiO_2	Standard Alneal (Best) Kerr and Cuevas [9]	n	1.5	1.7
SiO_2	Enhanced Alneal (Best) Current work	n	1	0.4
SiN_x	SiN_x Richter et al. [28]	n	1	0.64
AlO_x	AlO_x (ALD) Richter et al. [28]	n	1	0.26

deposited aluminium oxide (AlO_x), but this method requires the use of expensive dedicated equipment.

5. Charge transport during an enhanced alneal

To understand the rate at which the ionic charge was introduced, samples were annealed for various lengths of time before the interface charge concentration was measured. Cz, n-type Si, ~40 Ω cm, thermally oxidised to 100 nm was cleaved into samples of < 1 cm^2. These were deposited, at Oxford, with 100 nm thermally evaporated aluminium on one side and were annealed at 400 °C on a hot plate to allow greater control over the sample temperature and anneal time. After the anneal, the aluminium was removed, as was the back oxide. A contact was then made directly to the silicon using indium-gallium and conductive silver dag for the rear contact, and mercury probe capacitance-voltage (Hg-CV) measurements were performed to measure the charge at the Si/SiO_2 interface. It was found that ionic charge was present at the $Si\text{-}SiO_2$ interface after an anneal time of only minutes. Fig. 6 shows the interface charge after various anneal times at 400 °C in air on the hot plate.

The data in Table 1 shows that the high lifetimes achieved by the alneal incorporated a charge concentration of 1–2 × 10^{12} q/cm^2. From Fig. 6, a charge concentration of this magnitude is introduced at 400 °C in under 1 min. The interface charge concentration saturates after only a couple of minutes. This is believed to be due to the exhaustion of available ions. A standard alneal process is 30 min, so the introduction of these ionic species during the alneal is a much faster process. From the results of Fig. 6, an anneal of 30 min is not necessary to introduce charge and provide FEP. However, the migration of atomic hydrogen to the oxide-silicon interface may require the full length of the standard alneal but this cannot be concluded from present work. It is noted that movement of ions through 100 nm of oxide in a matter of minutes at 400 °C is remarkably fast and raises the question as to whether the process is purely diffusive. Indeed, when an as-oxidised sample from set B was annealed, without the presence of aluminium, the lifetime and CV measured interface charge was found to be unaffected. From previous work [49] and the literature on MOSFETs [50], it is known that once a Na or K contaminant resides within the silicon dioxide, the migration to the interface at 400 °C is very rapid. As no charge was seen after this anneal, it is likely that the contaminant does not reside within the oxide, but instead must enter from the oxide surface. This implies the following: either the ions were not present without the aluminium, i.e. that the process of evaporating the aluminium may be responsible for introducing the ions into the system, or that there was no driving force for the ions to overcome the activation energy to enter the oxide in the absence of an aluminium layer during the anneal. As the origin of the contamination was unclear, the importance and existence of a driving force on purposefully contaminated samples was investigated. It was hypothesised that the presence of aluminium, which has a work function lower than the silicon substrate, on the surface of the oxide, sets up an electric field within the oxide that causes injection of the ions into the oxide and their subsequent drift towards the silicon interface– a process which can be much faster than diffusion.

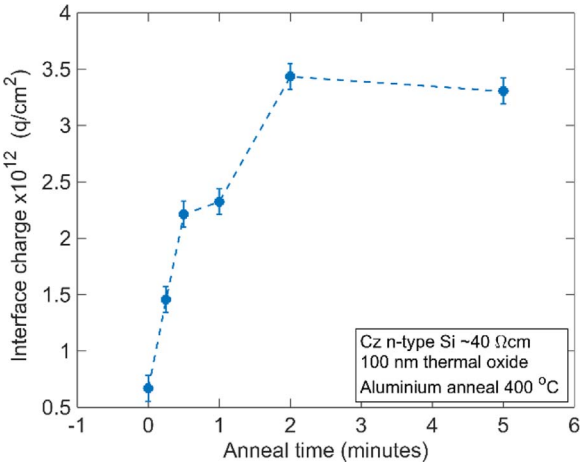

Fig. 6. Interface charge concentration $Q_{interface}$ after an aluminium anneal at 400 °C.

This hypothesis was tested by using a second metal with a work function *larger* than the silicon substrate so as to oppose, rather than drive, the movement of positive ions towards the $Si\text{-}SiO_2$ interface. Gold was used, due to its large work function of 5.1. To overcome the uncertainty regarding the source of the ions, a fraction of a monolayer of KCl was thermally evaporated onto the oxide surface, as in [49]. This ensured an ample supply of ionic charge was present when either metal top layer was used. Gold or aluminium were deposited on top of the KCl salts on 1 cm^2, 1 Ωcm, n-type, FZ samples. For the gold evaporation, a tungsten boat was used instead of a tungsten coil. These samples were then annealed on the hot plate at 400 °C for varying lengths of time. After this, the aluminium was removed using commercial etchant as previously, and the gold was removed using aqua regia (1 part nitric acid: 3 parts hydrochloric acid). The back oxides were etched off using HF and an ohmic contact to the silicon was created using InGa and conductive silver dag. This structure was suitable for Hg-CV measurements to be taken, to calculate the interface charge. The interface charge concentrations for the two different metals annealed for different lengths of time are shown in Fig. 7. Here it is evident that when Au is used, no charge is introduced into the oxide layer, whereas when Al is present significant quantities of charge are present at the $Si\text{-}SiO_2$ interface after the anneal.

In Fig. 7, when aluminium is used, charge is present at the interface

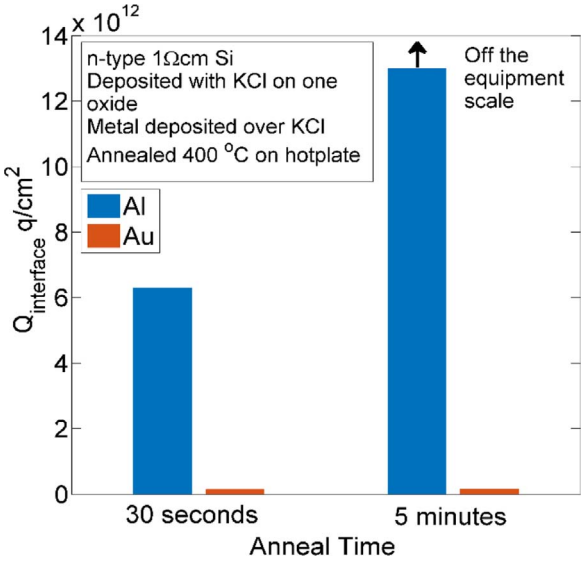

Fig. 7. Interface charge concentration for anneals of 30 s and 5 min at 400 °C on samples with KCl deposited on the oxide surface using either aluminium or gold during the anneal.

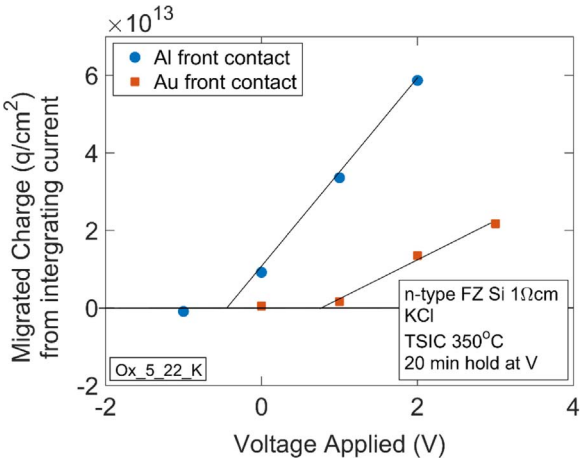

Fig. 8. Concentration of migrated charge, calculated by integration of TSIC current, against voltage applied during TSIC. The error in the measurement of charge is of the order of 10^{12} q/cm^2.

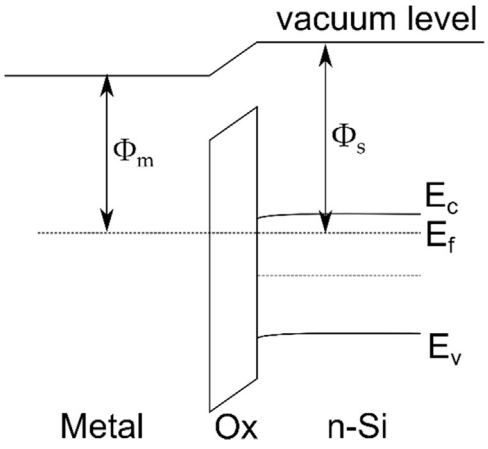

Fig. 9. Band diagram schematic to show work function difference and electric field created when aluminium is contacted to oxide passivated 1 Ω cm n-type silicon.

even after an anneal of only 30 s. A five minute anneal at this temperature increases the quantity of interface charge to be over the equipment measurement capability. However, the interface charge was not seen to increase, even after five minutes, when gold was used; instead it remained in the order of 1×10^{11} q/cm^2. This indicates that either the activation energy for the ions to leave the SiO_2-Au interface is greater than that of the SiO_2-Al interface, and/or there is not the same driving force enabling them to overcome the activation energy to enter the SiO_2. As K was introduced on purpose during these experiments, the magnitude of interface charge when an aluminium layer is used is one to two orders of magnitude greater than for the samples in Fig. 6 where no intentional ion deposition occurred.

MOS structures were fabricated on 1 Ω cm n-type FZ silicon for TSIC experiments. KCl salts were deposited before the metal front contact, as previously, to ensure a substantial source of ions. After the TSIC experiment the total migrated charge concentration was calculated from the recorded current as detailed in Section 2. The migrated charge, equivalent to the interface charge, is shown against TSIC voltage in Fig. 8. This shows that ions will migrate to the Si-SiO_2 interface when gold is the top contact metal, however a greater bias is necessary before the ions will drift to the interface.

When the 0 V bias condition of Fig. 8 is considered, for the Au contact, negligible charge is migrated after 20 min, whereas for the Al contact, a significant quantity of charge migrates ($> 1 \times 10^{13}$ q/cm^2), as is the case for the (unbiased) anneals shown in Fig. 7. Although no charge is introduced when gold is used in the zero bias condition, it is possible to migrate the K ions to the Si-SiO_2 interface when a larger voltage is applied. Extrapolation of the linear portion of the migrated charge versus bias voltage curves to zero migrated charge allows a threshold bias voltage to be identified. The Al intercept would indicate that ions migrate at bias voltages above −0.4 V, whereas the Au intercept demonstrates that a bias greater than +0.8 V is necessary before the K ions migrate, a difference between the two metals of 1.2 V. This difference is very similar to the work function difference between aluminium and gold. Work functions vary depending on lattice orientation and, according to the literature, range from 4.06–4.28 V for Al [51] and 5.1–5.5 V for Au [52].

It is speculated that during the enhanced alneal the work function difference between the silicon, which in the case of 1 Ω cm n-type doping is 4.32 V, and the aluminium ~4.1 V, $\Delta\Phi = 0.22$ V, is the driving force for the injection and drift of ions. A schematic of the band diagram is shown in Fig. 9 where Φ_{ms} is the metal-silicon work function difference, Φ_m is the metal work function and Φ_s is the silicon work function, dependant on doping concentration. The work function difference between the silicon and aluminium would increase with more highly resistive n-type material, or with p-type.

The aluminium work function is less than the silicon work function at this doping concentration, so the SiO_2 is subject to an electric field which favours the drift of positive ions towards the Si-SiO_2 interface. The result when using gold is different. Due to its work function being greater than the silicon substrate the field produced in the oxide will tend to oppose migration of ions to the silicon interface at zero bias and so account for the results in Figs. 8 and 9.

The Al-Si work function difference may seem small, but since the dielectric is only 100 nm thick, it results in an electric field of ~20 kV/cm which is quite sufficient to produce rapid ionic drift at elevated temperatures. Previous work has shown that once K and Na ions are within SiO_2 layers they are extremely mobile [49]. However, if the ions initially reside on the surface of the SiO_2, or at the interface of the SiO_2 with a metal, they must first be injected into the dielectric and this process is associated with a significant activation energy. It is this injection step that is thought to be rate limiting for the migration of K and Na across thin oxide films [53]. It is postulated that this activation energy is lowered by the electric field produced by the work function difference which thus allows rapid migration of the charge to the silicon interface.

The above results demonstrate that the potential of the top metal contact with respect to the silicon substrate is an important parameter in determining the kinetics of charge migration. It is thus interesting to consider what happens if an enhanced alneal is performed when the aluminium layer is *not* electrically connected to the silicon substrate. In this situation, as positively charged ions leave the aluminium interface and migrate towards the silicon substrate, a negative charge, and hence potential, will develop on the aluminium which will tend to oppose their movement. This negative potential will grow until no further movement of charge is possible, which according to Fig. 8 will require a potential of ~ −0.4 V and so will occur when a charge density of ~10^{11} q/cm^{-2} has accumulated on the 100 nm thick silicon oxide dielectric. This situation was implemented experimentally by depositing small aluminium dots on the oxide, 2 mm in diameter, in the centre of larger square specimens. The dots were left completely electrically unconnected to anything else whilst the enhanced alneal was performed at 400 °C. No KCl was intentionally deposited in this case. Subsequent measurements of charge did indeed show ~10^{11} q/cm^{-2} at the silicon interface as expected, see Fig. 10. Although it should be noted that such a charge concentration is not untypical of a thermal oxide and so does not necessarily lend weight to the hypothesis. If, on the other hand, the top aluminium layer is electrically connected to the silicon substrate no surface potential will be induced as ions migrate towards the silicon and so no opposing electric field will be developed. This situation was implemented experimentally in two different ways. The first was simply to deposit aluminium over the whole surface of the cleaved, oxidised

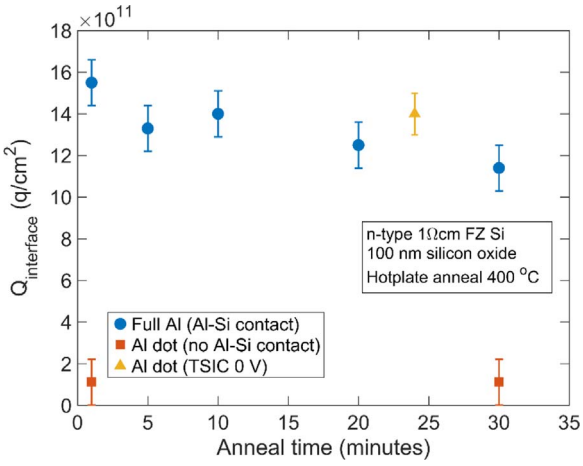

Fig. 10. Interface charge ($Q_{interface}$) calculated from CV measurements vs anneal time at 400 °C on hotplate. The anneals were conducted with the oxide surface either fully covered in aluminium (blue), or a 2 mm diameter aluminium dot in the centre of the oxide (orange). Error bars are shown as calculated in [54]. For comparison, a sample with an Al dot that underwent TSIC with a 0 V bias at 400 °C is included. (For interpretation of the references to colour in this figure legend, the reader is referred to the web version of this article.)

sample followed by an enhanced alneal at 400 °C with no KCl intentionally deposited. In this case ~10^{12} q/cm^{-2} was found at the silicon interface, presumably because there was sufficient leakage current between the aluminium layer and the substrate to prevent a significant build-up of potential. This current may have been due to the aluminium layer electrically contacting the silicon substrate at a cleaved edge of the sample or via pin holes in the oxide. The second way was simply to bias a 2 mm aluminium dot to 0 V so that its potential did not change, as shown by the yellow triangle in Fig. 10. In each case substantial charge was found to migrate to the silicon interface as shown in Fig. 10.

From this data, it is evident that when there is no electrical contact between the Al and Si, in the case of the Al dots, little ionic charge is introduced even after a 30 min anneal. However, when the Al covers the entire oxide surface, including a cleaved edge, charge concentrations of ~1.3 × 10^{12} q/cm^2, which are sufficient for enhanced alneal passivation are consistently introduced. In this case the specific amount of interface charge probably depends on the amount of unintentional K and Na contamination present in these experiments which will vary from specimen to specimen. When a sample with an Al dot is subjected to TSIC with a 0 V bias, charge of a similar quantity to that seen when a sample is annealed with the Al fully covering the oxide is evident at the Si-SiO_2 interface. As would be expected from the above explanation.

6. Conclusions

The passivation provided by one of the most effective passivation techniques, known as the alneal, has been improved by the addition of field effect passivation (FEP). This FEP has been added both extrinsically, by corona charge, and during the alneal process itself, in the form of ionic species present at the Si-SiO_2 interface. Low SRVs, routinely below 1 cm/s, with a lowest value of 0.4 cm/s, have been achieved on 1 Ωcm, n-type, FZ Si by means of this enhanced alneal which simultaneously introduced interface charge. SIMS measurements revealed that the species causing these low SRVs are likely to be Na and K ions, which are known to facilitate stable surface passivation. The introduction of charge is shown to happen in the order of minutes at 400 °C. It is proposed that the driving force to introduce these ions into the dielectric is the difference in the silicon and aluminium work functions. This creates an electric field in the dielectric that favours the migration of positive ions from the Al-SiO_2 interface to the Si-SiO_2 interface. This mechanism also accounts for the lack of substantial silicon interface charge when gold is used as a top contact or when the aluminium layer is electrically isolated from the silicon substrate.

Acknowledgments

K A Collett would like to thank EPSRC for funding her doctoral studies and the iMechE for the conference grant to attend SiliconPV. R S Bonilla is the recipient of an EPSRC (UK) Postdoctoral Research Fellowship, EP/M022196/1. P R Wilshaw and P Hamer acknowledge the support from EPSRC grant EP/M024911/1. Data published in this article can be downloaded from http://ora.ox.ac.uk. All authors are thankful to Martin Hermle and Christian Reichel at Fraunhofer ISE for provision of silicon material, and to Radka Chakalova for her extensive help in the cleanroom.

References

[1] B. L. Sopori, L. Jastrzebski, and T. Tan, A comparison of gettering in single and multicrystalline silicon for solar cells, Conference Rec. Twenty Fifth IEEE Photovolt. Spec. Conference, pp. 625–628 (1996).
[2] I. Périchaud, Gettering of impurities in solar silicon, Sol. Energy Mater. Sol. Cells 72 (2002) 315–326.
[3] M.A. Green, Solar Cells: Operating Principles, Technology and System Applications, Prentice-Hall, Englewood Cliffs, New Jersey, 1982.
[4] B. Sopori, X. Deng, J. Benner, A. Rohatgi, P. Sana, S. Estreicher, Y. Park, M. Roberson, Hydrogen in silicon: a discussion of diffusion and passivation mechanisms, Sol. Energy Mater. Sol. Cells 41–42 (. 1996) 159–169.
[5] P.C. Srivastava, U.P. Singh, Hydrogen in semiconductors, Bull. Mater. Sci. 19 (1) (1996) 51–60.
[6] J.E. Cotter, J.H. Guo, P.J. Cousins, M.D. Abbott, F.W. Chen, K.C. Fisher, P-type versus n-type silicon wafers: prospects for high-efficiency commercial silicon solar cells, IEEE Trans. Electron Devices 53 (8) (2006) 1893–1901.
[7] B. E. Deal, Measurement and control of dielectric film properties during semiconductor device processing, in Silicon Device Processing, Proceedings, Volume 13, 1970, pp. 36–50.
[8] M.J. Kerr, Surface, Emitter and Bulk Recombination in Silicon and Development of Silicon Nitride Passivated Solar Cells (PhD), The Australian National University, Canberra, Australia, 2002.
[9] M.J. Kerr, A. Cuevas, Very low bulk and surface recombination in oxidized silicon wafers, Semicond. Sci. Technol. 17 (2002) 35–38.
[10] J. Zhao, A. Wang, P.P. Altermatt, S.R. Wenham, and M.A. Green, 24% efficient silicon solar cells, in Proceedings of the IEEE First World Conference on Photovoltaic Energy Conversion (1994), pp. 1477–1480.
[11] A. Cuevas, P.A. Basore, G. Giroult-Matlakowski, C. Dubois, Surface recombination velocity of highly doped n-type silicon, J. Appl. Phys. 80 (6) (1996) 3370–3375.
[12] Y. Larionova, V. Mertens, N.-P. Harder, R. Brendel, Surface passivation of n-type Czochralski silicon substrates by thermal-SiO2/plasma-enhanced chemical vapor deposition SiN stacks, Appl. Phys. Lett. 96 (3) (2010) 32105.
[13] R.S. Bonilla, B. Hoex, P. Hamer, P.R. Wilshaw, Dielectric surface passivation for silicon solar cells: a review, Phys. Status Solidi (a) (2017) (In Press).
[14] M.J. Kerr, A. Cuevas, General parameterization of Auger recombination in crystalline silicon, J. Appl. Phys. 91 (3) (2002) 2473–2480.
[15] J. Zhao, A. Wang, P.P. Altermatt, M.A. Green, J.P. Rakotoniaina, O. Breitenstein, High efficiency PERT cells on n-type silicon substrates, in: Proceedings of the 29th IEEE Photovolt. Spec. Conference., no. 100 (2002), pp. 218–221.
[16] A.G. Aberle, Crystalline Silicon Solar Cells: Advanced Surface Passivation and Analysis, Centre for Photovoltaic Engineering, University of New South Wales, Sydney, 1999.
[17] P. Balk, Electrochemical Society Meeting, in Electrochemical Society Meeting (1965).
[18] Y.T. Yeow, D.R. Lamb, S.D. Brotherton, An investigation of the influence of low-temperature annealing treatments on the interface state density at the Si-SiO2 interface, J. Phys. D. Appl. Phys. 8 (1975).
[19] M. Reed, Models of Si-SiO2 interface reactions, Semicond. Sci. Technol. 4 (1989) 980.
[20] M.L. Reed, J.D. Plummer, Chemistry of Si-SiO2 interface trap annealing, J. Appl. Phys. 63 (12) (1988) 5776–5793.
[21] B.E. Deal, E.L. MacKenna, P.L. Castro, Characteristics of fast surface states associated with SiO2-Si and Si3N4-SiO2-Si structures, J. Electrochem. Soc. 116 (7) (1969) 997.
[22] G. Dingemans, F. Einsele, W. Beyer, M.C.M. Van de Sanden, W.M.M. Kessels, Influence of annealing and Al2O3 properties on the hydrogen-induced passivation of the Si/SiO2 interface, J. Appl. Phys. 111 (9) (2012) 93713.
[23] A.G. Aberle, Surface passivation of crystalline silicon solar cells: a review, Prog. Photovolt. Res. Appl. 8 (5) (2000) 473–487.
[24] R.S. Bonilla, K. Collett, L. Rands, G. Martins, R. Lobo, P.R. Wilshaw, Stable, extrinsic, field effect passivation for back contact silicon solar cells, Solid State Phenom. 242 (2015) 67–72.
[25] K.R. McIntosh, L.E. Black, On effective surface recombination parameters, J. Appl. Phys. 116 (1) (2014).
[26] K.L. Luke, L.J. Cheng, Analysis of the interaction of a laser pulse with a silicon wafer: determination of bulk lifetime and surface recombination velocity, J. Appl.

Phys. 61 (6) (1987) 2282–2293.
[27] A.B. Sproul, Dimensionless solution of the equation describing the effect of surface recombination on carrier decay in semiconductors, J. Appl. Phys. 76 (5) (1994) 2851–2854.
[28] A. Richter, S.W. Glunz, F. Werner, J. Schmidt, A. Cuevas, Improved quantitative description of Auger recombination in crystalline silicon, Phys. Rev. B - Condens. Matter Mater. Phys. 86 (16) (2012) 1–14.
[29] P.P. Altermatt, F. Geelhaar, T. Trupke, X. Dai, A. Neisser, E. Daub, Injection dependence of spontaneous radiative recombination in c-Si: Experiment, theoretical analysis, and simulation, NUSOD '05, in: Proceedings of the 5th International Conference Numer. Simul. Optoelectron. Devices, vol. 2005, no. 2 (2005), pp. 47–48.
[30] T. Trupke, M. a. Green, P. Würfel, P.P. Altermatt, a. Wang, J. Zhao, R. Corkish, Temperature dependence of the radiative recombination coefficient of intrinsic crystalline silicon, J. Appl. Phys. 94 (8) (2003) 4930–4937.
[31] D.B.M. Klaassen, A unified mobility model for device simulation-II. temperature dependence of carrier mobility and lifetime, Solid State Electron 35 (7) (1992) 961–967.
[32] PV Lighthouse. [Online]. Available: 〈https://www.pvlighthouse.com.au/〉.
[33] H. Mäckel, K. Varner, On the determination of the emitter saturation current density from lifetime measurements of silicon devices, Prog. Photovolt. Res. Appl. 21 (2013) 850–866.
[34] A. Kimmerle, J. Greulich, A. Wolf, Carrier-diffusion corrected J0-analysis of charge carrier lifetime measurements for increased consistency, Sol. Energy Mater. Sol. Cells 142 (2015) 116–122.
[35] R. Pässler, Semi-empirical descriptions of temperature dependences of band gaps in semiconductors, Phys. Status Solidi Basic Res 236 (3) (2003) 710–728.
[36] L.M. Terman, An investigation of surface states at a silicon/silicon oxide interface employing metal-oxide-silicon diodes, Solid. State Electron. 5 (5) (1962) 285–299.
[37] E.H. Nicollian, J.R. Brews, Metal Oxide Semiconductor — Physics and Technology, Wiley, New York, 1982.
[38] R.S. Bonilla, N. Jennison, D. Clayton-Warwick, K.A. Collett, L. Rands, P.R. Wilshaw, Corona charge in SiO2: kinetics and surface passivation for high efficiency silicon solar cells, Energy Procedia 92 (2016) 326–335.
[39] T.C. Kho, S.C. Baker-Finch, K.R. McIntosh, The study of thermal silicon dioxide electrets formed by corona discharge and rapid-thermal annealing, J. Appl. Phys. 109 (5) (2011).
[40] B.P. Rand, J. Genoe, P. Heremans, J. Poortmans, Solar cells utilizing small molecular weight organic semiconductors (February 2013, Prog. Photovolt. Res. Appl. 15 (2007) 659–676.
[41] R.S. Bonilla, G. Martins, P.R. Wilshaw, Investigation of parasitic edge recombination in high-lifetime oxidized n-Si, Solid State Phenom. 242 (2015) 73–79.
[42] J. Schmidt, A. Merkle, R. Brendel, B. Hoex, M.C.M. Van De Sanden, W.M.M. Kessels, Surface passivation of high-efficiency silicon solar cells by atomic-layer-deposited Al2O3, Prog. Photovolt. Res. Appl. 16 (2008) 461–466.
[43] W. Shockley, W.T. Read, Statistics of the recombinations of holes and electrons, Phys. Rev. 87 (5) (1952) 835–842.
[44] R.N. Hall, Electron-hole recombination in germanium, Phys. Rev. 87 (2) (1952) 387.
[45] W.D. Eades, R.M. Swanson, Calculation of surface generation and recombination velocities at the Si-SiO2 interface, J. Appl. Phys. 58 (11) (1985) 4267–4276.
[46] D.J. Fitzgerald, A.S. Grove, Surface recombination in semiconductors, Surf. Sci. 9 (2) (. 1968) 347–369.
[47] R.B.M. Girisch, R.P. Mertens, R.F. De Keersmaecker, Determination of Si-SiO2 interface recombination parameters using a gate-controlled point-junction diode under illumination, IEEE Trans. Electron Devices 35 (2) (1988) 203–222.
[48] A.G. Aberle, S. Glunz, W. Warta, Impact of illumination level and oxide parameters on Shockley-Read-Hall recombination at the Si-SiO2 interface, J. Appl. Phys. 71 (9) (1992) 4422–4431.
[49] R.S. Bonilla, P.R. Wilshaw, A technique for field effect surface passivation for silicon solar cells, Appl. Phys. Lett. 104 (2014).
[50] E.H. Snow, A.S. Grove, B.E. Deal, C.T. Sah, Ion transport phenomena in insulating films, J. Appl. Phys. 36 (5) (1965) 1664–1673.
[51] R.M. Eastment, C.H.B. Mee, Work function measurements on (100), (110) and (111) surfaces of aluminium, J. Phys. F. Met. Phys. 3 (9) (1973) 1738–1745.
[52] J.C. Rivière, The work function of gold, Appl. Phys. Lett. 8 (7) (1966) 172.
[53] M.R. Boudry, J.P. Stagg, The kinetic behavior of mobile ions in the Al-SiO2-Si system,", J. Appl. Phys. 50 (2) (1979) 942–950.
[54] L. Rands, Passivation of Silicon Surfaces Through the Introduction of Charge into Insulating Layers (Masters thesis), University of Oxford, Oxford, England, 2015.